SHADOW MODELING AND DETECTION FOR ROBUST FOREGROUND SEGMENTATION IN HIGHWAY SCENARIOS

Katherine Batista, Rui Caseiro and Jorge Batista
Institute of Systems and Robotics, DEEC-FCTUC, University of Coimbra, Portugal

Keywords: Foreground segmentation, Shadow modelling and detection, Traffic surveillance.

Abstract: This paper presents a method to automatically model and detect shadows on highway surveillance scenarios. This approach uses a cascade of two classifiers. The first stage of this method uses a weak classifier to ascertain the color information of possibly shadowed pixels which will be used by the second stage of this method (strong classifier). The weak classifier estimates the Color Normalized Cross-Correlation (*CNCC*) and the color information of the pixels identified as shadow, will be used to build or update multi-layered statistical shadow models of the RGB appearance of shadow. These models will then be used, by the strong classifier, to correctly distinguish shadow. To prevent misclassifications from corrupting the results of both classifiers, spatial dependencies are also taken into account. For this purpose, nonparametric kernel density estimators in a pyramidal decomposition (PKDE), as well as, Markov Random Fields (MRF) were independently employed. This technique is being used in a real outdoor traffic surveillance system in order to minimize the effects of cast vehicle shadows as well as shadows induced by illumination changes. Several results are presented in this paper to prove its effectiveness and the advantages of applying spatial contextualization methods to the weak and strong classifiers.

1 INTRODUCTION

Advances in camera technology as well as in scientific areas such as computer vision have lead to the development of efficient and robust real time traffic surveillance systems. In this sort of systems, the precise detection of moving objects is essential. Generally, most foreground segmentation processes (e.g. (Zhong and Sclaroff, 2003)) are sensitive to illumination changes or cast vehicle shadows which can lead to faulty detections which seriously reduces the efficiency of other dependent processes. More precisely, cast vehicle shadows can significantly increase the detected vehicle's area and lead to its merging with nearby vehicles. This fact gravely affects the outcome of any tracking or vehicle counting systems used in traffic surveillance. Illumination changes, induced by clouds or camera auto gain control processes can also generate false positives.

To overcome these problems, several methods have been developed where some are based on the use of color (e.g. (Cucchiara et al., 2003) or (Horprasert et al., 1999)), brightness, reflectance and geometry information to identify shadowed pixels. In (Cucchiara et al., 2003) shadows are identified by assuming that the difference of the hue and saturation components, between the pixel and corresponding background pixel, change within certain limits. Nonetheless, this technique is not flexible, seeing as it requires the prior definition of parameters which are not adaptable to illumination changes and are not constant for different scenarios. The authors in (Prati et al., 2003) also refer that this method presents low robustness in noisy scenarios. T. Horprasert (Horprasert et al., 1999) analyze the pixel's normalized brightness and normalized chromaticity distortions in the RGB color space and classifies a pixel as shadow using a set of thresholds. An automatic method is presented to estimate these limits, nonetheless, it is computationally too expensive to be used in a real time traffic surveillance system. Cavallaro (Cavallaro et al., 2005) also analyze pixel color information, yet in order to overcome the previously referred problems, combines this information with spatial constraints based on edge detection. However, this method doesn't remove shadows whose edge pixels are adjacent to objects and background pixels without the use of an heuristic analysis of a temporal shadow tracking procedure.

Other approaches use statistical models to learn and describe the appearance of cast shadow. For instance, Liu (Liu et al., 2007) use information obtained from a color based classifier and employ GMM (Gaussian Mixture Models) to model shadowed pixels in the HSV color space. To improve the classifier, they use

Batista K., Caseiro R. and Batista J. (2010).
SHADOW MODELING AND DETECTION FOR ROBUST FOREGROUND SEGMENTATION IN HIGHWAY SCENARIOS.
In *Proceedings of the International Conference on Computer Vision Theory and Applications*, pages 148-157
DOI: 10.5220/0002823401480157

local region level information to update these models. Brisson (Martel Brisson and Zaccarin, 2007) also use pixel color information in the YUV color space to build a Gaussian mixture shadow model (GMSM). Nevertheless, seeing as the approach is pixel-based, the obtained model's accuracy is dependent on the color-based classifier's results throughout time. In (Huang and Chen, 2008) shadows are identified by building pixel-based local region shadow models using GMMs. A global model is also estimated and used to update the local region models when movement is rare. The background, foreground and shadow models are built into a MRF energy function. However, this method's weak classifier which provides information for the learning of cast shadow, requires the definition of several parameters that are not adaptable to illumination changes.

On the other hand, Porikli (Porikli and Thornton, 2005) models shadows by multivariate Gaussians using RGB color information provided by a pre-filter. This approach does not require color space transformation and, seeing as it uses multiple independent layers to model each shadow pixel, it is more flexible than the standard GMMs approach to model shadow. The shadow models are achieved using color information provided by a pre-filter that evaluates color variation such as in (Horprasert et al., 1999). Shadow pixels are distinguished using these models and misclassification are corrected using shadow flow, which once again is a color-based analysis. One of the main drawbacks of this method, is the fact that it does not perform any sort of spatial contextualization of the pixel's label. Therefore, foreground pixels which possess similar color information to modeled shadow are misclassified.

The method here presented overcomes this flaw by considering that a pixel's label is influenced by its neighboring pixel labels. In a general matter, this method is composed by a cascade of two classifiers. To the results of these classifiers, spatial contextualization is induced to correct misclassifications. The first classifier is a weak classifier, which purpose is analyzing every segmented foreground pixel and determining whether a pixel is possibly shadow by measuring the similarity between color and texture of the foreground and corresponding background. This is done by estimating the Color Normalized Cross-Correlation (*CNCC*). This information is used to build or update statistical models that describe the RGB appearance of shadow pixels. These multi-layered pixel-based models are used by the second classifier (strong classifier) to identify cast shadows. Nonetheless, erroneous classifications may seriously compromise the foreground segmentation process. To minimize the number of misclassifications, the pixel's neighboring labels are taken into account. To do so, two distinct and independent approaches were implemented and compared. One, consists on a pyramidal decomposition of kernel density estimators (PKDE), which has as main goal ascertaining probabilistic representations of the surrounding pixel labels to improve the results given by the pre-filter. Another technique also analyzes the spatial label dependencies using a Markov Random Field (MRF) energy function which is minimized by the graph cut algorithm.

2 WEAK SHADOW CLASSIFIER

The weak classifier evaluates the segmented foreground pixels to determine whether a pixel is a possible shadow pixel. The main goal of this classifier is not to detect shadows accurately, but to filter out some impossible shadow pixels. The results of this classifier will be used further on by the strong classifier. The approach here presented estimates the *CNCC* between each segmented pixel I_t and the corresponding background pixel Bp_t (see subsection 2.1). To improve the results of this classifier, two distinct techniques were independently applied and compared. One, uses a PKDE method (presented in subsection 5.1), while another method ascertains the pixel's label by using a MRF approach (presented in subsection 5.2). A quantitative and qualitative analysis of the results of these two techniques can be found in subsection 6.1.

2.1 Color Normalized Cross-Correlation (*CNCC*)

This classifier measures the similarity of color and texture between foreground and background, by estimating the *CNCC* (Grest et al., 2003). More precisely, a pixel is classified as shadow if its texture is correlated with the corresponding texture of $Bp(t)$. In order to estimate the *CNCC*, the brightness information is split from the color values, which is done by representing the pixel's color in the bi-conic HSL space (Grest et al., 2003) (see Figure 1.(a)). To measure the similarity, the correlation between both can be estimated by projecting the RGB color vector onto the chromatic HS plane in order to calculate the Euclidean values of hue (h) and saturation (s). This allows the estimation of the scalar product between the referred pixels (h,s,L) which is proportional to their correlation. This is quite simple to understand, seeing as if they have similar hues (small angle between

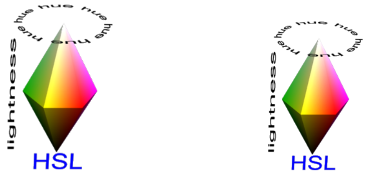

Figure 1: (a) Representation of the hue and saturation components of the HSL color space. (b) Chromatic plane of the hsL color space ($\vec{c^a}$ and $\vec{c^b}$ represent the projection of two color pixels on this plane).

them) and high saturations, the resulting correlation will be high (see Figure 1.(b)).

Hence, being c^F and c^B the color vectors, in the *hsL* space, of a foreground and background pixel at (x,y), the *CNCC* is estimated over a window $M \times N$ surrounding those pixels, using the following equation:

$$CNCC = \frac{\sum_{ij}(c^F_{xy} \bullet c^B_{xy}) - MN\overline{L^F}.\overline{L^B}}{\sqrt{VAR^F VAR^B}}; \quad (1)$$

where,

$$VAR^k = (\sum_{ij}(c^k_{xy} \bullet c^k_{xy}) - MN\overline{L^k}^2), \quad (2)$$

and $\overline{L^F}$ is the average intensity of the foreground pixels inside that window, $k \in \{F(foreground), B(background)\}$ and $(c^F_{xy} \bullet c^B_{xy}) = (h^F_{ij}, s^F_{ij}) \circ (h^B_{ij}, s^B_{ij}) + L^F_{ij} L^B_{ij}$, where the operator $\circ$ represents the scalar product. [1] For gray-level pixels, the *CNCC* will present similar values to the normalized cross correlation (*NCC*). The resulting values of *CNCC* lie within $[0 \ldots 1]$, which can be interpreted as probabilistic measurements, and the higher they present themselves, the more likely the pixel is a shadowed pixel. Consequently, a pixel can be identified as shadow if these values are larger than a given threshold. Several examples of results of this procedure are presented in Figure 2.

3 SHADOW MODELING

Shadow pixels can be distinguished by using statistical models of their RGB appearance. Basically, each image pixel possesses multiple layers, where each one of these, represent a different shadow appearance for that pixel. In this section, a method proposed in (Porikli and Thornton, 2005), is described to achieve these shadow models. The process becomes more discriminative the larger the number of layers. However,

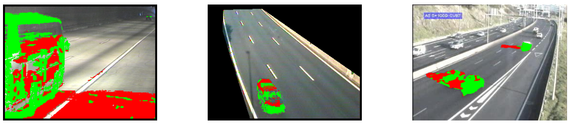

Figure 2: Results of the *CNCC* weak classifier (red=shadow, green=foreground).

seeing as this technique is meant to be applied in a real time system, a large number of layers may compromise the system's framerate. Thus, we chose to use three layers seeing as these proved sufficient to statistically describe the color information of shadow. Each one of these layers can be represented by a multivariate Gaussian distribution corresponding to each color channel. In other words, for every given pixel, three layers are estimated, where for each one of these layers, each RGB channel is modeled by a Gaussian distribution. To build or update a layer at a given time t, this method uses the RGB information ($x = [r,g,b]$) of a pixel identified as shadow by the weak shadow classifier. More precisely, to update a layer this method performs recursive Bayesian estimation using this information (Porikli and Thornton, 2005). Assuming the layer follows a normal-inverse-Wishart distribution, this update can be done using the following expressions:

$$\upsilon_t = \upsilon_{t-1} + n; \qquad \kappa_t = \kappa_{t-1} + n; \quad (3)$$

$$\theta_t = \theta_{t-1}\frac{\kappa_{t-1}}{\kappa_{t-1}+n} + \bar{x}\frac{n}{\kappa_{t-1}+n} \quad (4)$$

$$\begin{aligned}\Lambda_t = \Lambda_{t-1} + \Sigma^n_{i=1}(x_i - \bar{x}))(x_i - \bar{x}))^T + \\ +n\tfrac{\kappa_{t-1}}{\kappa_t}(\bar{x} - \theta_{t-1})(\bar{x} - \theta_{t-1})^T\end{aligned} \quad (5)$$

$$\Sigma_t = (\upsilon_t - 4)^{-1}\Lambda_t \quad (6)$$

where, v_t and Λ_t are the degrees of freedom and scale matrix for inverse Wishart distribution, θ_t the mean, Σ_t the covariance and κ_{t-1} the number of prior observations. When the update is performed at each time frame (i.e. $n = 1$), the mean of the new samples, $\bar{x}$, becomes the pixel's color information x. These parameters are re-estimated when a layer is updated and they describe the pixel's appearance by combining the prior information with the new color information. When each layer is initialized, the following parameters are assumed (Porikli and Tuzel, 2005): $\kappa_0 = 10$; $\upsilon_0 = 10$; $\theta_0 = x_0$; $\Lambda_0 = (\upsilon_0 - 4)16^2 I$; where I is a three dimensional identity matrix.

Each layer has also associated a confidence measurement, given by: $C = \frac{\kappa_t^3(\upsilon_t-2)^4}{(\upsilon_t-4)|\Lambda_t|}$, which decreases with larger variances. This parameter is used in the layer update algorithm, by sorting the three different

[1] The negative values are set to zero.

Algorithm 1: Layer update algorithm.

```
Input:
  1. All pixels identified as foreground;
  2. $L_i$ = different layers ($i = 1,...,NUM\_LAYERS$);
for All pixels identified as foreground: do
    1. $x = [r,g,b]$ = pixel identified as shadow by the
       weak shadow classifier;
    2. Sort layers $L_i(\theta_{t-1}, \Sigma_{t-1}, \upsilon_{t-1}...)$ according to
       confidence measurements.
    3. for $i \leq NUM\_LAYERS$ do
           (a) Estimate Mahalanobis distance:
               $d_i = (x-\theta_{t-1,i})^T \Sigma_{t-1,i}^{-1} (x-\theta_{t-1,i})$;
           (b) if
           ($Sample\ x\ in\ 99\%\ confidence\ interval$)
               • Update layer $L_i$ model parameters
           (eq. 3
               4, 5 and 6);
               • Analyze next Pixel $x$;
               else
               • Decrease the number of observations:
                 $\kappa_t = \kappa_{t-1} - n$;
               endif
       end
    4. if $No\ layer\ updated$ :
           Delete layer $L$ with lowest confidence
           measurement and initialize new layer with
           new sample and new initial parameters.
       endif
end
```

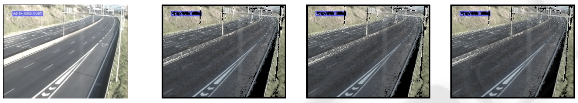
(a) (b) (c) (d)

Figure 3: Background image represented in (a) and the corresponding shadow models (ordered from most confident to least confident (b) to (d)).

layers according to their variances. The layer updating process is recapitulated in algorithm 1. Figure 3 shows several examples of different shadow models for a shadowy scenario.

4 SHADOW /FOREGROUND SEGMENTATION

Foreground pixels are those that are not identified as background or shadow. The process used to estimate the background model is not exploited in this paper, however for more details see (Monteiro et al., 2008). Having statistically modeled the color appearance of shadow it is possible to correctly identify the shadow and true foreground pixels. To do so, the different shadow layers are sorted accordingly to their confidence measurements and the Mahalanobis distance is calculated between the pixel's color and each layer.

Unlike (Porikli and Thornton, 2005), a pixel is not immediately labelled as shadow if its color information lies within the 99% confidence interval of one of the shadow model layers. This would lead to erroneous classifications due to noisy less confident layers.

Algorithm 2: Shadow classifier algorithm (Strong Classifier).

```
Input:
  1. $L_i$ = different shadow layers
     ($i = 1,...,NUM\_LAYERS$);
  2. $C_{min}$ =Minimum normalized confidence
     (threshold);
  3. $C_{\sum min}$ =Minimum sum of normalized confidence
     (threshold);
for All pixels identified as foreground ($x = [r,g,b]$)
do
    1. Sort layers $L_i(\theta_{t-1}, \Sigma_{t-1}, \upsilon_{t-1}...)$ according to
       confidence measurements.
    2. for $i \leq NUM\_LAYERS$ do
           (a) Estimate Mahalanobis distance;
           (b) if ($x\ in\ 99\%\ confidence\ interval$)
               • Normalize the $L_i$
                 confidence measurement: $C_{norm_i}$.
               • Re-estimate the layer's sum of
                 normalized confidence:
                 $C_{sum} = C_{sum} + C_{norm_i}$
           endif
       end
    3. if ( The layer's $C_{norm_i} \geq C_{min}$
       and $C_{sum} \geq C_{\sum min}$)
           • Pixel classified as shadow.
       endif
    4. if ($Above\ conditions\ not\ satisfied\ for\ no\ L_i$):
           • Pixel classified as foreground.
       endif
end
```

The method here presented avoids labeling as shadow, pixels that lie within the confidence interval of low confident shadow models. To do so, each pixel's layer confidence is normalized ($C_{norm_i} = \frac{C_i}{\sum_i Ci}$) and the sum of normalized confidence measurements of model layers with which the sample is within the 99% confidence interval $C_{\sum norm}$ is estimated. If one of these values is lower than two thresholds (i.e. $C_{norm_i} < C_{min}$ or $C_{\sum norm} < C_{\sum min}$, where $C_{min} = \frac{1}{NUM\_LAYERS}$ and the default $C_{\sum norm} = 0.5$), then the pixel is not labeled as shadow. This is done mainly to avoid noisy less confident models from inducing erroneous classifications in the segmentation process. In subsection 6.2 a quantitative analysis is presented to prove the benefits of introducing these thresholds (C_{min} and $C_{\sum min}$) in this procedure.

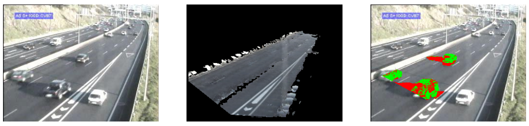

Figure 4: (a) Captured image. (b) Most confident shadow model. (c) Results of the strong classifier.

Vehicle pixels which possess similar color information as the shadow models can be mislabelled as shadow (which can be seen in Figure 4.(c)). To overcome this drawback, spatial context can be introduced into this final classification.

5 SPATIAL CONTEXTUALIZATION METHODS

By using the pixel's neighboring label information it is possible to minimize the number of wrongly classified pixels. For this purpose, two distinct techniques were independently employed and compared. One, uses a PKDE approach (presented in subsection 5.1), while another method ascertains the pixel's label by using a MRF approach (presented in subsection 5.2). A quantitative and qualitative analysis of the results of these two techniques can be found in subsection 6.1 and 6.2.

5.1 Pyramidal Decomposition of Nonparametric Kernel Density Estimators (PKDE)

The main goal of this method, is to use statistical representations of the surrounding pixel labels to correct erroneous classifications. Having to chose a model and estimate the distribution parameters is avoided using nonparametric kernel density estimators (KDE). Therefore, the distribution's probability density function (pdf) can be given by:

$$p(z) = \frac{1}{N}\sum_{i=1}^{N} K_h(z - z_i) \qquad (7)$$

where, N represents the number of data points and K_h is a kernel function with bandwidth h. Choosing a Gaussian kernel function, the density model can be achieved by placing a Gaussian over each data point and adding up the contributions over the whole data set and normalizing it by dividing this result by the number of data points (Bishop, 2006), which gives:

$$p(z) = \frac{1}{N}\sum_{i=1}^{N} \frac{1}{(2\pi h^2)^{1/2}} e^{\left\{\frac{-\|z-z_i\|^2}{2h^2}\right\}} \qquad (8)$$

Given the fact we are statistically modeling a pixel's classification based on its neighboring information, the pdf is estimated for a two dimensional domain space and therefore z becomes $z = [x\ y]$. The resulting two dimensional kernel density model can then be represented by:

$$p(z) = \frac{1}{N}\sum_{i=1}^{N} \frac{1}{2\pi(\det\Sigma)^{1/2}} e^{-\frac{1}{2}\left([z-z_i]^T\Sigma^{-1}[z-z_i]\right)} \qquad (9)$$

where, Σ is the covariance matrix.

By estimating the pdf functions over a M by M window surrounding the pixel ($N = M \times M$), the pixel's label is ascertained. The choice of an appropriate kernel function's bandwidth, h is rather tricky. If it is too small the kernel density model will be undersmoothed but, on the other hand, if it is too large it will become over-smoothed. Several automatic bandwidth selector methods have been developed throughout the years, such as MISE (mean integrated square error) or AMISE (asymptotic MISE) driven methods (Wand and Jones, 1994). Oversmoothing, least squares cross-validation, biased cross-validation or plug-in methods are several examples of AMISE bandwidth estimator techniques. These methods are computationally too expensive for real time systems or require the specification of a pilot bandwidth (plug-in methods). Nonetheless, simpler methods have emerged, such as the balloon estimator (Mittal and Paragios, 2004), where the bandwidth is calculated in function of the distance from the point to the nearest data point. However, this method is subject to discontinuities and integration at infinity problems. Another strategy, known as sample point estimator, calculates the bandwidth in function of the sample points (Mittal and Paragios, 2004). However, in the method here proposed, the bandwidth is obtained using a procedure similar to the one proposed in (Mittal and Paragios, 2004), and is calculated as the covariance of the data within the $M \times M$ window ($h = \Sigma$). By doing this, areas with larger uncertainty will be given less weightage in the pdf function. To minimize the influence of the size of this $M \times M$ window, a pyramidal image structure is used, where multi-scaled subsampling is preformed on the probabilistic data. It is important to state that the KDE's bandwidth and probabilities are calculated for each level of the pyramidal structure in order to prevent over or under smoothing. The probabilities of a pixel being shadow or foreground are then analyzed in a logarithmic scale and the pixel's label is finally ascertained.

5.1.1 PKDE Applied to the Results of the Weak Classifier

Using the *CNCC* classifier's results, a pixel can be identified as shadow when the estimated *CNCC* is larger than a given threshold. This threshold can be empirically set accordingly to the desired shadow detection rate, i.e. a high threshold will sub-detect shadow, while a low one will over detect it. However, threshold driven classifiers are bound to lead to misclassifications, such as the ones represented in Figure 2. To prevent these erroneous classifications from corrupting the statistical models, the pixel spatial dependencies are analyzed. The result of applying the PKDE technique to the results of the *CNCC* weak classifier are exemplified in Figure 5.

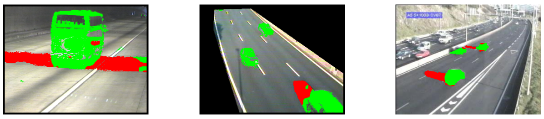

Figure 5: Examples of this weak classifier's (*CNCC*+PKDE) results.

5.1.2 PKDE Applied to the Results of the Strong Classifier

To improve the results of the strong classifier, the PKDE (presented in subsection 5.1) was employed. Figure 6 shows an example of the outcome produced by this method.

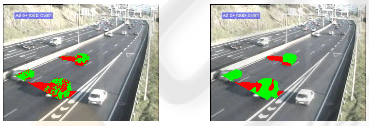

Figure 6: (a) Strong classifier Results. (b) PKDE applied to the strong classifier results.

5.2 Markov Random Fields (MRF)

Segmentation is a typical vision problem that can be naturally expressed in terms of energy minimization. More specifically, problems that require the estimation of spatially varying quantity (intensity, texture) from noisy measurements, can be formulated in a Bayesian framework using MRF. Spatial context is an important constraint when making decisions about a pixel's label, i.e., a pixel's label is not independent of the pixels neighborhood labels. So, instead of using only likelihood information of models, MAP (maximum *a posteriori*)-MRF framework provides a convenient prior for modelling this spatial interaction. This fact allows a global inference to be made, using local information, since labels conditional independence rarely exists between proximal sites. The objective is to assign a binary label l_p from the set $l_p \in \{foreground, shadow\}$ to each of the sites $p \in P$, where P is the set of segmented pixels, and $L = \{l_p | p \in P\}$ is the global labelling field of random variables (or configuration of the field). The goal is to find a L configuration, which minimize a energy function. In our case the function considered belongs to F^2 class of energy functions, defined in (Kolmogorov and Zabih, 2004) as a sum of function of up to two binary variables at a time. Seeing as it satisfies the conditions proposed in (Kolmogorov and Zabih, 2004) the optimization of L can be achivied by finding the minimum cut of a capacitated graph. First order MRF energy function can be decomposed as follows:

$$E(L) = \sum_{p \in P}[D_p(l_p) + \sum_{q \in N_p} V_{p,q}(l_p, l_q)] \quad (10)$$

where $D_p(l_p)$ is the term derived from the observed data that measures the cost of assigning the label l_p to the pixel p (evaluates the likelihood of each pixel belonging to one of the two classes), $V_{p,q}(l_p, l_q)$ measures the cost of assigning the labels l_p , l_q to the adjacent pixeis p, q, and is used to impose spatial smoothness (spatial coherence of labels throught a pairwise interaction MRF prior, by penalizing discontinuities between neighboring pixels), and N_p is the set of interacting pairs of pixeis (eight-connected neighboring). In a real time system, the computation time is a crucial factor, Greig (Greig et al., 1989) showed that the MAP solution of a two label pairwise MRF can be efficiently obtained in polynomial time by finding the st-mincut on the equivalent graph, providing an exact global optimial solution. The prior takes the form of the Ising model, a particular case of the generalized Potts model, for two label problems. The piecewise constant smoothness prior is used to stress spatial context, by assigning penalties for label discontinuities between neighboring pixels. The penalty used does not depend on the assigned labels, as long as they are different, and is spatially invariant. The data cost term $D_p(l_p)$, is defined as the negative log likelihood of a pixel p belonging to foreground or shadow class. In the following sections, we will show how to determine these likelihoods, when MRF is applied to the weak or to the strong classifier. Graph cut techniques from combinatorial optimization can be used to find the global minimum for a multidimensional energy function. MAP estimate of a MRF can be obtained by solving a multiway minimum cut problem on a graph. The minimum s/t cut problem can be solved by finding a maximum flow from the source s to the sink t (Boykov and Kolmogorov, 2004), so energy function of equation 10 can be efficiently minimized by the graph cut algorithms. The minimum cut of the graph can be computed through a variety of approaches, like the Ford-Fulkerson algorithm (Ford and Fulkerson, 1962), but in our case we performed the cut using the min-cut/maxflow algorithm, based on augmenting paths formulated by Kolmogorov (Boykov and Kolmogorov, 2004).

5.2.1 MRF Applied to the Results of the Weak Classifier

The *CNCC* weak classifier provides results that can be taken as independent probabilistic measurements for the pixel's label. Thus, these results can be used as the likelihood of a pixel's label in the MRF energy function. In this case, the procedure does not require the definition of thresholds. Figure 7 shows several examples of the application of this technique.

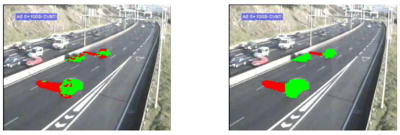

Figure 7: (a) Weak *CNCC* Classifier results. (b) Weak Classifier + MRF results.

5.2.2 MRF Applied to the Results of the Strong Classifier

To apply the MRF approach, the sum of normalized confidences of layers with which the sample lies within the confidence interval, is used as the likelihood of the pixel's label. The higher this sum presents itself, the more likely the pixel is indeed a shadow pixel and therefore, it provides a spatial independent probabilistic measurement for that pixel's label. Figure 8 shows several results of applying this techniques to the results of the model driven shadow classifier.

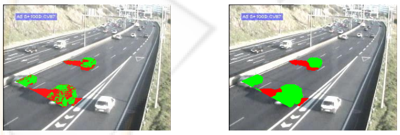

Figure 8: (a) Strong Classifier results. (b) Strong Classifier + MRF results.

6 RESULTS

Table 1: η and ξ rates of several weak classifier methods for three different thresholds.

	Thresholds					
	0.3		0.5		0.7	
Methods	η	ξ	η	ξ	η	ξ
CNCC	88.0	74.0	76.7	90.6	54.3	97.9
CNCC+KDE	88.1	75.6	76.8	91.3	53.9	98.2
CNCC+PKDE	83.6	88.9	71.6	97.6	41.6	99.7
CNCC+MRF	78.3	96.6	78.3	96.6	78.3	96.6

To analyze the effectiveness of this method, ground truth shadow and foreground pixels were identified on a sequence of 450 frames of a highway scenario. Not all vehicles were identified, only the ones on the lanes closest to the surveillance camera. In this section several results of applying these methods to this sequence are presented. To evaluate the accurateness of each method, the metrics presented in (Prati et al., 2003) are used to estimate the rates of false positives and negatives. More precisely, to measure the number of false negatives (i.e. shadow pixels wrongly classified as foreground) the shadow detection rate η is estimated and to measure the false positives (i.e. foreground pixels classified as shadow) the shadow discrimination rate ξ is calculated, using the following expressions:

$$\eta = \frac{TP_S}{TP_S+FN_S} \qquad \xi = \frac{\overline{TP_F}}{TP_F+FN_F} \qquad (11)$$

where, TP is the number of true positives (pixels correctly classified), FN is the number of false negatives, $\overline{TP_F}$ is the number of ground-truth points of the foreground objects minus the number of points detected as shadows, but belonging to foreground objects, while F and S represent foreground and shadow, respectively.

This section is composed of two main parts, where the first presents a quantitative and qualitative analysis of the performance of the weak shadow classifier. In the second part, the same analysis is performed for the results obtained by the overall process for foreground segmentation and shadow detection.

6.1 Weak Shadow Classifier Results

In this subsection, the performance of four independent weak shadow classifier methods are compared. The first is the result of estimating each pixel's *CNCC* and classifying it as shadow if this value is above a pre-defined threshold. The second method employs a kernel density estimator (*KDE*) to the results of this classifier, while the third applies the PKDE approach. The last uses the estimated *CNCC* in a MRF framework. To analyze the outcome of these methods, three different thresholds where applied and their performances compared.

Table 2: η and ξ rates obtained by taking or not into account thresholds (C_{min} and $C_{\sum min}$).

	Strong Classifier	
	η	ξ
No thresholds	94.4	69.4
Thresholds	87.7	80.1

The weak classifier's main goal is to correctly identify as many shadow pixels as possible. Therefore, the aim is to achieve a high shadow discrimination rate, ξ, seeing as it indicates a low number of false positives. The shadow detection rate, η, is as well important seeing as if it is low, the shadow models will take too long to converge. Analyzing the results obtained for the threshold driven methods (*CNCC*, KDE, PKDE) presented in Table 1, it is possible to see a clear improvement using the KDE approach and an even higher ξ using the PKDE technique. However, the shadow detection rate is clearly low in this last method (41.59%). It is important to state that these methods are threshold driven and their performances are clearly dependent of the defined threshold. Therefore, the wisest choice for this weak classifier is the MRF approach, seeing as its efficiency does not rely on the chosen threshold and its ξ and η are quite high (96.6% and 78.3% respectively).

6.2 Foreground/Shadow Segmentation Results

The main goal of a good shadow classifier is too achieve high ξ and η. The results presented in this section were achieved throughout the final 100 frames of the test sequence, seeing as the first 350 where used to estimate the multi-layered shadow models. This was done in order to correctly evaluate the impact of using these models in the shadow classification process. Due to all the reasons explained in subsection 6.1, the chosen weak classifier is the MRF approach. Table 2 presents the results obtained by the foreground segmentation process (Strong Classifier which corresponds to algorithm 2) when thresholds (C_{min} and $C_{\sum min}$) are taken into account.

The performance of this classifier improves significantly by introducing these thresholds, seeing as ξ increases, which indicates a lower percentage of foreground pixels identified as shadow. The shadow detection rate η decreases slightly but is, nevertheless, still quite high (87.7%).

Introducing spatial context to the results of this strong classifier, several misclassifications are going to be corrected, namely, false positives induced by pixels belonging to vehicles that present similar color information as the shadow models. Table 6.3 presents the results of independently applying the KDE technique, as well as the PKDE estimator and yet, the MRF approach to the results of the strong classifier. Examining this table, it is possible to see that employing the PKDE and MRF techniques to the results of the strong classifier, ξ increases and therefore, the percentage of false positives is reduced significantly. Comparing more thoroughly the results of both these methods, it is possible to see that the PKDE procedure presents a higher ξ (lower percentage of false positives) but a lower η when compared with the MRF approach. Figure 9 shows an example of this behavior.

Table 3: η and ξ rates for the Strong Classifier methods using the last 100 frames.

Methods	η	ξ
Strong Classifier	87.68	77.06
Strong Classifier+KDE	89.10	79.65
Strong Classifier+PKDE	83.01	94.34
Strong Classifier+MRF	91.91	84.50

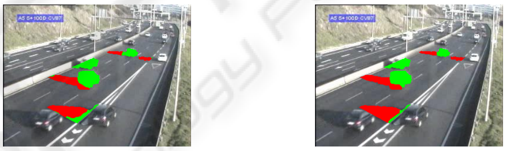

(a) PKDE approach (b) MRF approach

Figure 9: Results of Strong Classifier associated with PKDE and MRF approaches.

However, both methods present good detection rates and can be efficiently applied to induce spatial context to the results given by the strong classifier.

Nonetheless, a qualitative analysis of both methods indicates that the MRF approach preforms a more accurate spatial contextualization than the PKDE technique.

To support this claim, a quantitative interpretation was made by applying the Distance Transform to images containing the ground truth and classified foreground and shadow pixels. The distance transform sets each image pixel as the distance to the nearest boundary pixel. Therefore false positives located in the outmost regions of the blob will possess lower distance transform values seeing as these are closer to the nearest boundary pixel. By comparing these values and the one obtained for the ground truth, it is possible to ascertain an estimate on the errors of the spatial contextualization made by each method. Table 6.4 presents the shadow detection and shadow discrimination rates obtained using the equations in expression 11, but considering the distance transform values instead of the actual number of true positives or false negatives. As expected, η and ξ of the MRF

Table 4: Spatial context efficiency analysis of the strong classifier techniques (using the Distance Transform).

Methods	η	ξ
Strong Classifier	93.05	77.17
Strong Classifier+KDE	94.27	80.30
Strong Classifier+PKDE	88.36	95.69
Strong Classifier+MRF	95.90	93.95

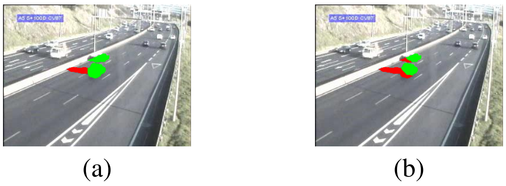
(a) (b)

Figure 10: (a) Weak classifier + MRF results. (b) Strong Classifier + MRF results.

technique are quite high.

Nevertheless, the PKDE is computationally less expensive than the MRF process, which is an important factor in a real time surveillance system. Looking at the results given by the weak classifier (present in Table 1), one question may arise: what is the need of statistical shadow models, seeing as this classifier already presents acceptable results? Yet, it is possible to see that using a strong classifier aided by the MRF technique, clearly improves the shadow detection rate η, which means that the percentage of false negatives is significantly reduced. Although the number of false positives increased, these are mainly located on the borders of the blobs and do not significantly deteriorate the vehicle segmentation process. An example of this behavior is shown in Figure 10 where, due to the non identification of shadow, it is possible to see that the leftmost vehicle's area is remarkably larger, when employing only the weak classifier.

The Distance transform was applied to carry out the same spatial context analysis performed previously. Looking at the results presented in Table 6.5, it is possible to conclude that this technique identifies shadow more accurately, seeing as, in a global matter, the weak classifier identifies less shadow which can lead to discontinuous blobs or blobs with considerably larger areas.

7 CONCLUSIONS

This paper presented an automatic method to identify cast vehicle shadow. This method pre-identifies shadow pixels and uses their color information to develop multi-layered statistical models that describe the RGB appearance of shadow. These shadow models were used to correctly label shadow pixels. To overcome misclassification, two independent processes (PKDE and MRF), that induce spatial context to the results of the classifiers, were employed and compared. The PKDE technique presented acceptable results and is computationally less expensive than the MRF approach. Nevertheless, its results proved to be slightly poorer than the MRF approach, which is also threshold invariant and therefore a more reliable approach. In order to employ this technique in a real time highway surveillance system, multiprocessing systems were used in its implementation. The method was thoroughly tested on a highway scenario sequence, where the ground truth foreground and shadow pixels were identified. The obtained results are quite satisfactory (91.91% shadow detection rate and 84.5% shadow discrimination rate).

Table 5: Spatial context efficiency analysis of the strong classifier and weak classifier techniques (using the Distance Transform).

Methods	η	ξ
Weak Classifier + MRF approach	90.40	98.20
Strong Classifier + MRF approach	95.90	93.95

REFERENCES

Bishop, C. M. (2006). *Pattern Recognition in Machine Learning*. Springer.

Boykov, Y. and Kolmogorov, V. (2004). An experimental comparison of min-cut/max- flow algorithms for energy minimization in vision. *Pattern Analysis and Machine Intelligence, IEEE Transactions on*, 26(9):1124–1137.

Cavallaro, A., Salvador, E., and Ebrahimi, T. (2005). Shadow-aware object-based video processing. *IEEE Proceedings - Vision, Image and Signal Processing*, 152(4):398–406.

Cucchiara, R., Grana, C., Piccardi, M., and Prati, A. (2003). Detecting moving objects, ghosts, and shadows in video streams. *IEEE Transactions on Pattern Analysis and Machine Intelligence*, 25(10):1337–1342.

Ford, L. R. and Fulkerson, D. R. (1962). *Flows in Networks*. Princeton University Press.

Greig, D. M., Porteous, B. T., and Seheult, A. H. (1989). Exact maximum a posteriori estimation for binary images. *Royal Statistical Soc., Series B*, 51:271–279.

Grest, D., michael Frahm, J., and Koch, R. (2003). A color similarity measure for robust shadow removal in real time. In *Proc. of Vision, Modeling, and Visualization (VMV)*.

Horprasert, T., Harwood, D., and Davis, L. S. (1999). A statistical approach for real-time robust background subtraction and shadow detection. In *ICCV Frame-Rate WS*.

Huang, J. B. and Chen, C. S. (2008). Learning Moving Cast Shadows for Foreground Detection. In *The Eighth International Workshop on Visual Surveillance - VS2008*, Marseille France. Graeme Jones and Tieniu Tan and Steve Maybank and Dimitrios Makris.

Kolmogorov, V. and Zabih, R. (2004). What energy functions can be minimized via graph cuts? *IEEE Transactions on Pattern Analysis and Machine Intelligence*, 26:147–159.

Liu, Z., Huang, K., Tan, T., and Wang, L. (2007). Cast shadow removal combining local and global features. *Computer Vision and Pattern Recognition, IEEE Computer Society Conference on*, 0:1–8.

Martel Brisson, N. and Zaccarin, A. (2007). Learning and removing cast shadows through a multidistribution approach. *IEEE Trans. Pattern Anal. Mach. Intell.*, 29(7):1133–1146.

Mittal, A. and Paragios, N. (2004). Motion-based background subtraction using adaptive kernel density estimation. volume 2, pages II–302–II–309 Vol.2.

Monteiro, G., Marcos, J., Ribeiro, M., and Batista, J. (2008). Robust segmentation for outdoor traffic surveillance. In *ICIP*, pages 2652–2655.

Porikli, F. and Thornton, J. (2005). Shadow flow: A recursive method to learn moving cast shadows. *Computer Vision, IEEE International Conference on*, 1:891–898.

Porikli, F. and Tuzel, O. (2005). Bayesian background modeling for foreground detection. In *ACM International Workshop on Video Surveillance and Sensor Networks (VSSN)*, pages 55–28.

Prati, A., Mikic, I., Trivedi, M. M., and Cucchiara, R. (2003). Detecting moving shadows: Algorithms and evaluation. *IEEE Transactions on Pattern Analysis and Machine Intelligence*, 25(7):918–923.

Wand, M. P. and Jones, M. C. (1994). *Kernel Smoothing (Monographs on Statistics and Applied Probability)*. Chapman & Hall/CRC.

Zhong, J. and Sclaroff, S. (2003). Segmenting foreground objects from a dynamic textured background via a robust kalman filter. *Computer Vision, IEEE International Conference on*, 1:44.